JOURNAL OF MATERIALS SCIENCE 29 (1994) 3738–3742

Transformation studies of M- to W-type hexaferrite in $BaFe_{12-2x}Co_{3x}O_{19}$

S. K. MANDAL, K. SINGH, D. BAHADUR
Metullurgical Engineering and Materials Science Centre, Indian Institute of Technology, Powai, Bombay 400076, India

Samples of general formula $BaFe_{12-2x}Co_{3x}O_{19}$ ($x=0.1$, 0.3, 0.5) have been synthesized by ceramic as well as citrate gel routes. The X-ray diffraction patterns indicate that M-type phase forms for $x=0.1$, while W-type phase is favourable for $x=0.3$ and 0.5. The results for $x=0.3$ are particularly interesting. While the X-ray diffraction data show evidence of a monophasic W-type hexaferrite, the magnetic, thermal and microstructural investigations indicate a secondary phase presumably at grain boundaries. Transformation of M- to W-type hexaferrite has been explained in terms of different possibilities such as nucleation of secondary phases, formation of vacancies and different site occupation of ions in the structure.

1. Introduction

M- and W-type hexaferrites have been studied extensively because of their wide applications and easy synthesis [1–3]. The two structures are closely related. While their *a*-axes are essentially the same, they vary in the *c*-parameter. In W-phase, two successive R-blocks ($BaFe_6O_{11}$) are interspaced by two S-blocks ($Me_2Fe_4O_8$) instead of one in the case of M-type hexaferrite. It has been recently reported that Ba–W hexaferrite can be obtained in M-type stoichiometry by using a suitable nucleating agent and/or hot-pressing technique [4, 5]. We report here an investigation of the development of W-type hexaferrite in a nominal composition $BaFe_{12-2x}Co_{3x}O_{19}$ ($0 \leqslant x \leqslant 0.5$) by essentially adding excess cobalt in M-type stoichiometry. Samples have been synthesized through the citrate gel precursor route to enable nucleation and growth to occur at reasonably low temperatures [6]. By varying the heat-treatment schedule, conversion of M- to W-type hexaferrite has been investigated. For comparison, the ceramic route has also been used. The results based on the structural and magnetic characterization are presented here.

2. Experimental procedure

AR grade chemicals were used to synthesize $BaFe_{12-2x}Co_{3x}O_{19}$ ($0 \leqslant x \leqslant 0.5$) through the citrate gel route. Citrate complexes involving Ba^{2+} and Co^{2+} ions were prepared by adding excess citric acid to the barium nitrate and cobalt nitrate solutions. The resultant solutions were mixed with stoichiometric quantities of ferric ammonium citrate solution by adding this solution slowly while stirring continuously. The pH of the solution was maintained at about 8 by adding ammonia solution. The mixed solution was then refluxed at 340 K for 24 h. Thereafter the citrate complex was dried at about 350 K, to obtain the precursor. Thermogravimetric analysis (TGA) of the precursor was carried out up to a temperature of 1270 K to determine the decomposition behaviour of the precursor. It was found that all the decomposition occurs up to about 670 K. Beyond 670 K, the precursor exhibits essentially constant weight. The precursor was then heated at 870 K for 24 h for its decomposition. The obtained powder was ground, pelletized and heat treated at temperatures of 1170, 1370 and 1570 K for 4 h each. The samples obtained through the ceramic route were given a final heat treatment at 1570 K. Final heat-treated samples were characterized for their crystal structure and phase by X-ray diffraction (XRD) (Philips PW-1729 X-ray generator and PW-1710 diffractometer control). Magnetic measurements were carried out using PAR 150A vibrating sample magnetometer. Scanning electron micrographs were taken on Jeol JSM 840A. TGA and differential scanning calorimetry (DSC) were performed with the help of Du Pont Instruments 910 (DSC) and 951 (TGA) for a few samples to have some

TABLE I Sample codes of the various samples synthesized by the citrate gel and ceramic routes. Compositions marked * are synthesized by the conventional ceramic route. The citrate route samples were presintered at 870 K, while for the ceramic samples the calcination temperature was 1370 K

	Sample composition; x in $BaFe_{12-2x}Co_{3x}O_{19}$	Heat-treatment temperature (K) for 4 h	Sample codes
1	0.0	1170	G9
2	0.0	1370	G11
3	0.1	1170	1G9
4	0.1	1570	1G13
5	0.3	1170	3G9
6	0.3	1370	3G11
7	0.3	1570	3G13
8	0.3*	1370	3C11
9	0.3*	1570	3C13
10	0.5	1170	5G9
11	0.5	1370	5G11
12	0.5	1570	5G13

0022–2461

idea regarding decomposition and phase transition. Table I gives the details of heat-treatment schedules and codes of the various samples synthesized.

3. Results and discussion

Fig. 1 gives the XRD patterns of sample $BaFe_{12-2x}Co_{3x}O_{19}$ for $x = 0.5$ synthesized by the citrate gel route and heat treated at different temperatures. Although the as-prepared citrate precursor is amorphous, the sample heat treated at 870 K is a mixture of crystalline γ-Fe_2O_3 and some amorphous phase. On the other hand, the sample heated at 1170 K (5G9) shows the presence of α-Fe_2O_3, M-type and W-type hexaferrite phases. However, samples

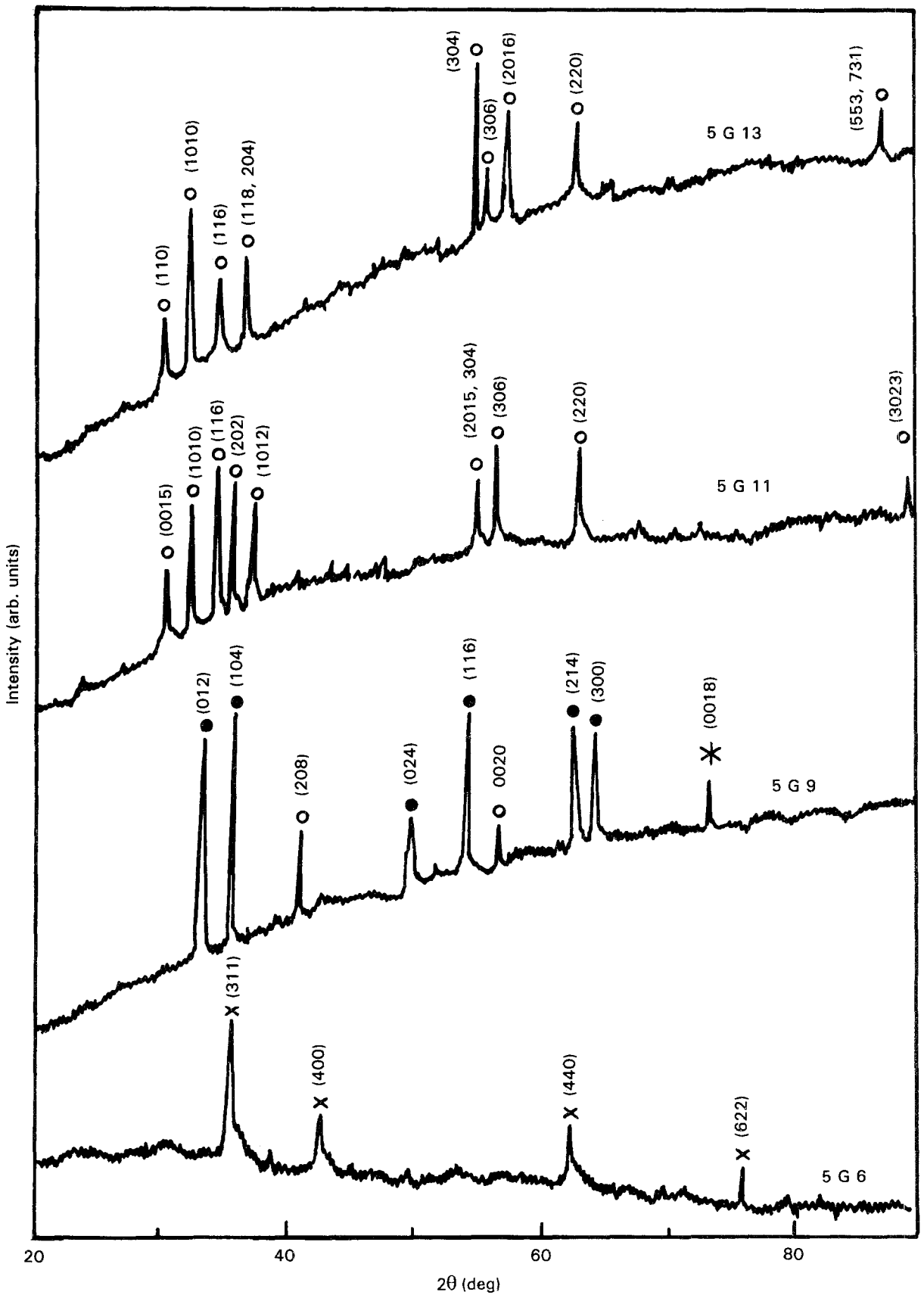

Figure 1 X-ray diffraction patterns for samples 5G6, 5G9, 5G11 and 5G13. (○) $BaCo_2Fe_{16}O_{27}$, (*) $BaFe_{12}O_{19}$, (●) α-Fe_2O_3, (×) γ-Fe_2O_3.

5G11 and 5G13 exhibit only W-type hexaferrite phase. The sample with $x = 0.3$ shows essentially a similar behaviour, but for the sample with $x = 0.1$ heated to 1570 K, only M-type phase is seen instead. Fig. 2 compares the XRD patterns of samples 1G13, 3G13 and 5G13. Table II compares the d-values for the four strongest lines of the samples 3C13 and 3G13 with the standard values. It is interesting to note that the XRD pattern of samples synthesized by the citrate gel route and heated to 1570 K differ considerably from that of the sample synthesized through the ceramic route. For example, the XRD intensity patterns of samples 3G13 and 3C13 are quite different. Most of the high-angle lines are absent in the diffraction pattern of the ceramic sample. This would indicate different site occupation of the cations when the material is synthesized through different routes. The lattice parameters of the samples calculated from the XRD data match those of M-type hexaferrite for some samples as given in Table III, but match those of W-type for some other samples. It may be mentioned that both M- and W-type ferrites have a similar hexagonal structure.

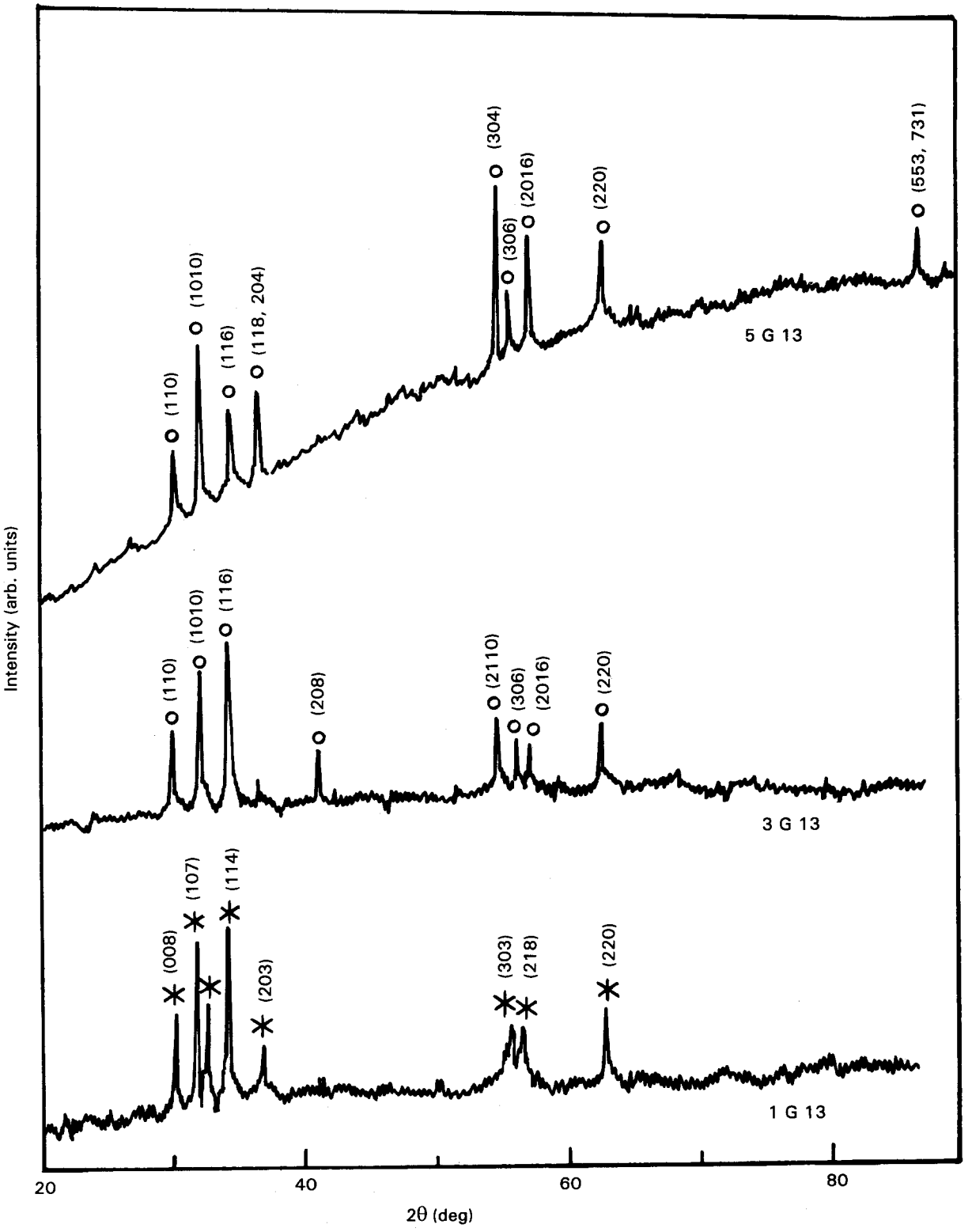

Figure 2 X-ray diffraction patterns for samples 1G13, 3G13 and 5G13. (●) $BaCo_2Fe_{16}O_{27}$, (*) $BaFe_{12}O_{19}$.

TABLE II Comparison of d-values of 3G13 and 3C13 with the standard d-values

3G13		3C13		Standard	
d-values (nm)	I/I_0	d-values (nm)	I/I_0	d-values (nm)	I/I_0
0.295	52	–	–	0.295 (1 1 0)	40
0.277	75	0.275	48	0.276 (1 0 1 0)	70
0.260	100	0.259	54	0.259 (1 1 6)	100
0.147	47	0.147	96	0.147 (2 2 0)	NA
–	–	0.113	100	0.113 (2 0 2 6)	NA

NA, not available.

TABLE III Magnetic properties, lattice parameters and particle size of some of the presently synthesized samples

Sample	Magnetization at ~ 12 kOe (e.m.u. g^{-1})	H_c (Oe)	T_c(K)	a(nm)	c(nm)	Particle size (μm)
G9	50.6	5170	–	0.588	2.314	1.7
G11	51.8	1950	–	0.591	2.219	1.8
1G9	37.2	3150	716	0.587	2.313	0.5
1G13	59.2	130	715	0.582	2.359	0.6
3G9	43.2	2170	717	0.588	2.318	0.8
3G11	58.0	165	–	0.587	3.302	–
3G13	53.7	130	533, 713	0.591	3.280	1.5
3C13	57.3	60	748	0.590	3.294	–
5G11	41.9	1280	–	0.593	3.267	–
5G13	63.7	110	763	0.590	3.281	–

The difference between the two lies in different c values ($c \simeq 23.2$ and 32.8 nm, respectively, for M- and W-type) [7]. The magnetization obtained at a magnetic field of about 12 kOe, the coercive field, H_c, and estimated Curie temperatures from magnetization versus temperature data along with the lattice parameters calculated for the different samples, are given in Table III. Fig. 3 shows a typical hysteresis loop for samples 3G9 and 3G13. These plots do not show evidence of complete saturation. The indication of non-saturation in samples could be due to large magnetocrystalline anisotropy which needs a higher field for saturation. Further, the nonsaturation in sample 3G9 could also be due to the presence of α-Fe_2O_3 which is canted antiferromagnet and can give rise to this kind of behaviour. This could also explain the reduction in magnetization values at the maximum field of 12 kOe. The coercivity shows a decreasing trend with increasing heat-treatment temperature which could be due to transition from single-domain to multidomain particles which is related to magnetization reversal changes from coherent rotation to domain wall motion. The remanent magnetization is also much larger for sample 3G9 than 3G13, indicating some kind of orientation effect.

We have plotted magnetization versus temperature for samples 3G9, 3G13, 5G13 and 3C13 in Fig. 4 as

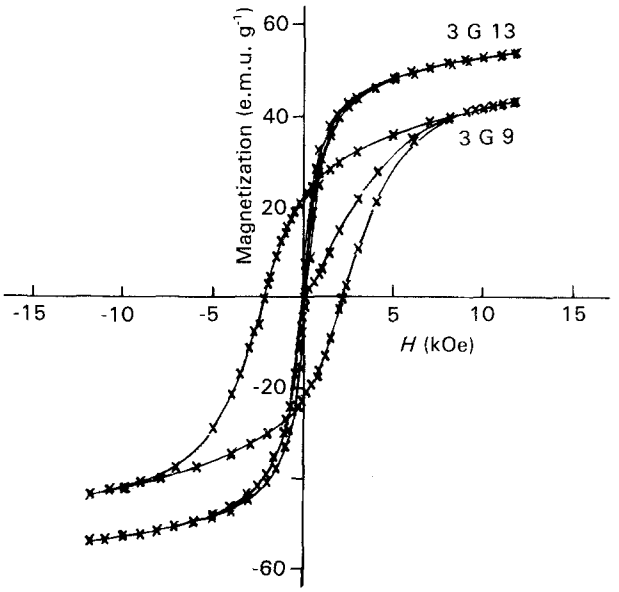

Figure 3 Room-temperature hysteresis loops for samples 3G9 and 3G13.

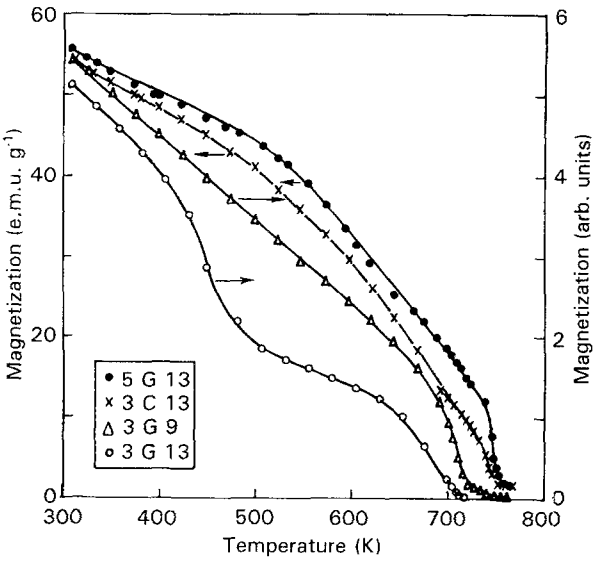

Figure 4 Magnetization versus temperature curves for samples (△) 3G9, (×) 3C13, (●) 5G13 and (○) 3G13. Measurements for samples 3C13 and 5G13 were taken at fields of 6 and 5 kOe, respectively, whereas those for 3G9 and 3G13 were taken at residual fields.

typical data. All the samples except sample 3G13 exhibit a single transition between 710 and 760 K, as is expected of a single hexaferrite phase. Sample 3G13, on the other hand, displays a second transition around 530 K. It may be pointed out that this sample shows the presence of W-type hexaferrite only in its XRD pattern. It is also noteworthy that there is fairly a large difference in the transition temperature between 3C13 and 3G13.

Fig. 5 shows a typical set of microstructures for samples 3G9 and 3G13. The presence of very fine particles and secondary phases is evident from the microstructure of the sample 3G9 which supports the XRD and magnetization data. The microstructure for sample 3G13 exhibits larger well-formed particles with a single-phase W-type hexaferrite. There is some indication of a secondary phase along the grain

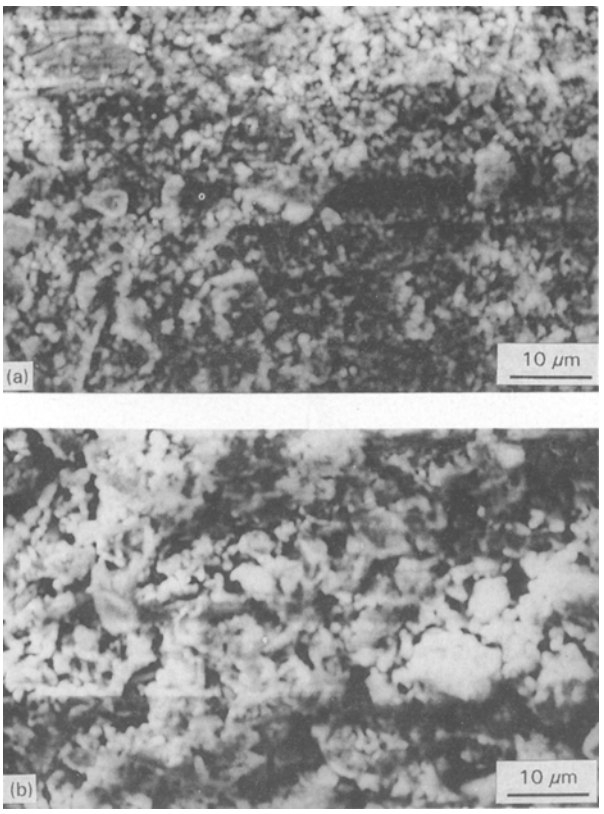

Figure 5 Scanning electron micrographs of (a) sample 3G9, and (b) sample 3G13.

boundaries, which is not detectable by XRD, perhaps due to very small volume fraction.

The evidence of a single-phase W-type hexaferrite from XRD and two transitions in M versus T data for the sample 3G13 is quite interesting. The initial nominal composition for this sample corresponds to $BaFe_{11.4}Co_{0.9}O_y$ which is quite different for a W-type hexaferrite, $BaCo_2Fe_{16}O_{27}$. The formation of W-type hexaferrite would obviously require more cobalt and iron cations which are not available. Hence this possibility is ruled out. The samples synthesized by the citrate route are initially heat treated at 870 K. It has been reported that at low temperatures secondary phases such as α-Fe_2O_3 and $BaFe_2O_4$ may nucleate which later react at high temperatures to form single-phase $BaFe_{12}O_{19}$ [8]. Therefore, a second possibility to support the formation of W-phase could be that a secondary phase related to $BaFe_2O_4$ might nucleate at 870 K so that the required ratio of Ba: (Fe + Co) for W-phase is available in the remaining material. The present XRD results do not indicate the presence of any such phase, and show a monophasic W-type hexaferrite. However, the magnetic and SEM data support the presence of a secondary phase. An additional magnetic transition (Fig. 5) is observed at around 530 K in addition to one observed at around 720 K due to the W-phase) which could be attributed to a secondary phase along the grain boundaries. DSC analysis supports these results. The DSC curve of sample 3G13 shows essentially two broad transitions: the first one is around 515 K while the other one is around 720 K. These transitions correspond fairly well with the magnetic transition temperatures observed. The additional magnetic transition, however, is not found in the ceramic sample of the same composition because the secondary phase might not have been nucleated as the samples are heated initially at high temperature (1370 K). The situation where the citrate route sample forms W-type hexaferrite with nucleation of some secondary phases whereas the ceramic sample forms W-type hexaferrite without nucleation of any such phases, could be explained as follows. The high-temperature calcination of the ceramic sample might force some of the Ba^{2+} ions also to go to the Co^{2+} sites in the W-phase as $Ba[Co_2]Fe_{16}O_{27}$. As mentioned earlier the unit cell of W-type phase is closely related to the M-phase. The only difference is that the successive R-blocks are interspaced by two S-blocks instead of one, as in the M-phase. The divalent cations (Ba^{2+}) could, in principle, replace Co^{2+} ions in the spinel blocks [5]. A large number of divalent cations have been found suitable for this replacement [3, 9–11]. Here the Ba^{2+} ions may distribute themselves between R and S blocks in order to obtain a stoichiometry corresponding to the W-phase.

The W-phase obtained by the present method could also be due to non-stoichiometry by the presence of a number of vacant Fe^{3+}/Co^{2+} sites in the compound. The XRD pattern does not show all the peaks corresponding to the various interplanar spacings. This is believed to be due to vacancies in such planes [5].

The nucleation and growth mechanism of W-type hexaferrite for citrate and ceramic samples appears to be different.

Acknowledgements

The authors thank the Council of Scientific and Industrial Research (CSIR), India for financial support, and Mr S. V. Sharma (I.I.T. Kanpur) for carrying out some magnetic measurements.

References

1. B. J. SHIRK and W. R. BUESSEM, *J. Am. Ceram. Soc.* **54** (1970) 192.
2. D. BAHADUR and D. CHAKRAVORTY, in "Proceedings of ICF-5" C. M. Srivaslava and M. J. Patni, (Oxford and IBH, Delhi, 1989) p. 189.
3. J. P. MINGOT, P. WOLFERS and J. C. JOUBERT, *J. Magn. Magn. Mater.* **51** (1985) 337.
4. S. RAM, D. BAHADUR and D. CHAKRAVORTY, *ibid.* **67** (1987) 378.
5. P. BRAMHA, A. K. GIRI, M. ROY, D. BAHADUR and D. CHAKRAVORTY, *ibid.* **103** (1992) 174.
6. A. SRIVASTAVA, P. SINGH and M. P. GUPTA, *J. Mater. Sci.* **22** (1987) 1489.
7. J. SMIT and H. P. J. WIJN, "Ferrites" (Wiley, New York, 1959) p. 177.
8. F. CHOU, X. FENG, J. LI and Y. LIU, *J. Appl. Phys.* **61** (1987) 3881.
9. K. U. I. JISHENG, L. U. HUAIXIAN and D. U. YOUWEI, *J. Magn. Magn. Mater.* **31–34** (1983) 801.
10. J. P. MINGOT, A. COLLOMB and J. C. JOUBERT, *ibid.* **58** (1986) 239.
11. A. COLLOMB, O. ABDEKADAR, P. WOLFERS, J. C. JOUBERT and D. SAMARAS, *ibid.* **58** (1986) 247.

Received 22 June
and accepted 10 December 1993